Highly Selective and Sensitive Determination of Pb(II) Ions Using Ion Selective Electrodes (ISE) Coated with the BEC6ND1 Ionophore as Membranes

Nasriadi Dali [1,*], Armadi Chairunnas [2], Hilda Ayu Melvi Amalia [3]

[1]   Department of Chemistry, Faculty of Mathematics and Natural Sciences, Halu Oleo University, Kendari 93232 - Southeast Sulawesi, Indonesia; nasriadidali@ymail.com (N.D.);

[2]   Department of Biology, Faculty of Mathematics and Natural Sciences, University of Nahdlatul 'Ulama Sulawesi Tenggara, Kendari 93563 - Southeast Sulawesi, Indonesia; armadisajami@gmail.com (A.C.);

[3]   Study Program of Tadris Biology, Faculty of Tarbiyah and Teacher Training, Institut Agama Islam Negeri (IAIN), Kendari 93563 - Southeast Sulawesi, Indonesia; hildaayumelvi@gmail.com (H.A.M.A.);

*   Correspondence: nasriadidali@ymail.com (N.D.);

Abstract: The research on determining highly selective and sensitive Pb(II) ions using ion-selective electrodes (ISE) coated with the BEC6ND1 ionophore as a membrane has been successfully carried out. ISE was designed using a membrane composition [(BEC6ND1 ionophore : PTCPB : DOS : PVC) (3 : 2 : 60 : 35 % w/w)]. The ISE-BEC6ND1 ionophore has good characteristics where it shows a sensitivity value of 29.395 mV/decade in the Pb(II) ion concentration range of 10^{-9} - 10^{-1} M with a limit of detection (LoD) 10^{-7} M. The response time is 4 - 8 minutes, with a relative standard deviation (RSD) of 0.21. The ESI-BEC6ND1 ionophore also shows the average value of selectivity coefficient (K_{ij}) < 1. These results indicate that the presence of Fe(II), Zn(II), and Cd(II) ions as interfering ions in the analyte solution does not affect the performance of the ESI-BEC6ND1 ionophores in detecting Pb(II) ions. The ESI-BEC6ND1 ionophore that has been developed shows good selectivity, sensitivity, stability, and reproducibility, so the ESI-BEC6ND1 ionophore is promising to be used as a Pb(II) ion detector in the environment.

Keywords: BEC6ND1 ionophore; calix[6]arene; ISE-Pb(II); membrane; selective.

1. Introduction

Lead (Pb) is a heavy metal toxic to the body. Pb toxins can enter the human body through the respiratory tract, digestion, and skin layer penetration. Pb that is absorbed through the respiratory tract, digestive tract and skin will be transported by the blood to all organs and tissues of the body. About 95% of Pb is bound by erythrocytes, and 5% of Pb is bound by blood plasma. About 30-40% of Pb that is absorbed through the respiratory tract will enter the bloodstream and lungs for circulation to all organs and tissues of the body. About 10-30% of Pb that is absorbed through the digestive tract will enter the organs and tissues of the body [1-3].

Prolonged exposure to Pb can cause disturbances in various body organ systems, such as the nervous, gastrointestinal, urinary, and hematopoietic systems. The nervous system is the most sensitive system to Pb toxins. The tetraethyl lead compound [$Pb(C_2H_5)_4$] is an antinock additive used in petrol. This compound can cause acute poisoning in the central nervous

system, although the poisoning process occurs in a long time with a small absorption rate. Diseases related to the brain as a result of Pb poisoning are encephalopathy (swelling of the brain) and delirium (mental disorders), which are characterized by hallucinations, epilepsy, coma, seizures, headaches, eye irritation, blindness, tumors, cancer, nervous system disorders, decreased immunity, and death. Clinical symptoms that often occur in the digestive tract system due to lead poisoning are small intestinal colic, which is always accompanied by severe constipation, namely localized pain around the umbilicus. Pb compounds that enter the urinary system (kidneys) can cause kidney damage. The damage is caused by the formation of intranuclear inclusion bodies and the formation of aminoaciduria, namely the occurrence of excess amino acids in the urine. Clinical symptoms that often occur in the hematopoietic system due to Pb poisoning are disturbances in heme biosynthesis. Blood Pb levels of 10 μg/dL can inhibit the activity of the enzyme δ-aminolevulinate dehydratase (ALAD) in bone marrow erythroblasts and erythrocytes. This can increase urinary and serum levels of δ-aminolevulinate (ALA). High levels of ALAD can cause neurotoxicity. Blood Pb levels of 40-50 μg/dL can cause disturbances in hemoglobin synthesis. Meanwhile, blood Pb levels of 70 μg/dL can cause clinical anemia [1-3].

Clinical symptoms caused by exposure to Pb in various organs and body tissues cause Pb levels in the environment to be monitored regularly. The methods of determining Pb in environmental samples that are widely used today are Atomic Absorption Spectrometry (AAS), Laser-Induced Breakdown Spectroscopy [4,5], Flame Atomic Absorption Spectrometry (FAAS) [6-12], Inductively Coupled Plasma Mass Spectrometry (ICP-MS) [13], Fluorescence Resonance Energy Transfer (FRET) [14], Ion Chromatography [15], and Voltammetry methods [16-18]. These various analytical methods require instruments whose prices and operational costs are very expensive, so these instruments are not available at every institution, even though the institution requires them concerning waste monitoring. Therefore, we need to develop a Pb metal analysis method with a low price and operational cost, but this instrument has high quality, sensitivity, and selectivity.

An ion-selective electrode (ISE) is a chemical sensor widely used to determine cation and anion ions [19-22]. This is because the ISE method has advantages such as (1) an analysis by ISE quickly and accurately, (2) ISE can measure the activity of a species directly, (3) ISE has high selectivity so that it does not require separation, (4) range of comprehensive measurement, and (5) analysis cost of cheap [23].

The use of calix[n]arene derivatives as ionophores in ISE membrane components can increase the selectivity of potentiometric electrodes [24]. This is because calix[n]arene has a basket-like structure, so these compounds can be used to interact with ions or neutral molecules [25]. In addition, the derivative compound calix[n]arene also has a unique functional group so that it can interact selectively with heavy metal ions. Research results related to this are the use of *p-tert*-butylcalix[4]arene and *p-tert*-butylcalix[4]-and-[6]arene thioamides as ionophores on the surface of the coated wire electrode (CWE) for the analysis of the Pb(II), Hg(II), and Au(I) ions [26,27]. The use of the BEC4ND1 ionophore as a membrane on ISE-Hg(II) also showed very high selectivity and sensitivity to Zn(II), Cd(II), and Pb(II) ions [28-33]. Therefore, it is necessary to study selectivity testing ISE-Pb(II) with tetra(p-tert-butyl)tetra(ethylester)calix[6]arene or BEC6ND1 ionophore as membrane against the Fe(II), Zn(II), and Cd(II) ions.

In this study, we report a new method for determining Pb(II) ions using the BEC6ND1 ionophore as a membrane at an ion-selective electrode (ISE). We found that using the

BEC6ND1 ionophore as a membrane in ISE showed highly selective and sensitive results for the determination of Pb(II) ions. Therefore, the ESI-BEC6ND1 ionophore is expected to be used as a Pb(II) ion detector in an environmental sample.

2. Materials and Methods

2.1. Apparatus and materials.

The apparatus used is analytical balance (Explorer Ohaus), avometer digital multimeter ACDC UT89XD (Uni-T), chemical beaker (Pyrex), dropper pipette (Pyrex), funnels (Pyrex), hot plate magnetic stirrer SH-2 (Faithful), magnetic stirrers (1 cm), measuring cup (Pyrex), micropipette (Pyrex), oven laboratorium UN110 (Memmert), round bottom flask (Pyrex), scientific orion star A321 pH meter (Thermo Fisher), stand cooler (Pyrex), stirring rod, stopwatch analog 505 (Diamond). The FTIR spectrum was recorded in KBr powder on a Shimadzu® FTIR Prestige-21 spectrometer (Shimadzu Corporation, Kyoto, Japan).

The materials used are Ag wire, aquabidest (Onelab Waterone), a blue tip, $Cd(NO_3)_2$ p.a. (Merck), Cu wire, parafilm "M" (Pechiney), $FeSO_4$ p.a. (Merck), $Pb(NO_3)_2$ p.a. (Merck), plasticizer dioctyl sebacate (DOS), poly(vinyl chloride) (PVC) (Fluka), potassium tetrakis(4-chlorophenyl borate) (PTCPB) (Aldrich), Pt wire, Sn wire, tetrahydrofuran p.a. (THF) (Merck), and $Zn(NO_3)_2$ p.a. (Merck). The BEC6ND1 ionophore was synthesized using the method reported Dali [34].

2.2. Characterization of the ISE-BEC6ND1 ionophore by FTIR.

The ISE-BEC6ND1 ionophore synthesized from Dali [34] was characterized by an FTIR spectrometer.

2.3. Design of the ISE-BEC6ND1 ionophore.

The electrode body is made of a blue tip tube with a diameter of 2 mm and a length of 7 cm. A platinum (Pt) electrode with a diameter of 0.2 mm and a length of 2 cm is connected to a copper (Cu) wire using a lead (Sn) wire solder. The Pt electrode is inserted into the electrode body. The top and bottom of the electrode body were wrapped with parafilm as retaining Cu and Pt wires. The bottom of the Pt electrode is left exposed so it can be coated with a membrane. The Pt electrode was immersed in a membrane solution with the composition [ISE-BEC6ND1 ionophore : PTCPB : DOS : PVC (3 : 2 : 60 : 35% w/w)] for 24 hours [27].

2.4. Nernst (sensitivity) factor of the ISE-BEC6ND1 ionophore.

The potential value of the Pb(II) solution (10^{-9} - 10^{-1} M) was measured using the ISE-BEC6ND1 ionophore. The potential value was measured while the Pb(II) solution (10^{-9} - 10^{-1} M) was stirred with a magnetic stirrer to remove air bubbles on the membrane surface. The measurement results are graphed between the potential value of E (mV) as the y-axis and -log Pb(II) as the x-axis. The sensitivity value (S) of the ISE-BEC6ND1 ionophore is obtained from the regression coefficient b from the linear regression Equation (1). At the same time, the K value is obtained from the regression coefficient a from the linear regression Equation (1) by extrapolating the linear curve to the y-axis [35].

$$\hat{y} = a + bx \quad .... \quad (1)$$

2.5. Detection limit of the ISE-BEC6ND1 ionophore.

The detection limit of the ISE-BEC6ND1 ionophore was determined by constructing an exponential curve on the linear regression lines of the Nernstian and non-Nernstian. The intersection point of the exponential curve on the linear regression line shows the concentration limit of the ISE-BEC6ND1 ionophore detection limit [36].

2.6. Precision of the ISE-BEC6ND1 ionophore.

ISE-BEC6ND1 ionophore precision was measured as relative standard deviation (RSD) using Equation 2:

$$RSD = \frac{SD}{\bar{x}}$$ .... (2)

where SD is the standard deviation, and ẍ is the average of the measurements [37].

2.7. Response time of the ISE-BEC6ND1 ionophore.

The response time of the ISE-BEC6ND1 ionophore was determined from the length of time required to produce a constant potential value of the Pb(II) solution (10^{-9} - 10^{-1} M).

2.8. Selectivity of the ISE-BEC6ND1 ionophore.

The ISE-BEC6ND1 ionophore selectivity coefficient was determined using the matching potential method (MPM). The potential value of the Pb(II) solution (10^{-9} - 10^{-1} M) (main ion) was measured using the ISE-BEC6ND1 ionophore in the absence of interfering ions. Furthermore, the potential value of the Pb(II) solution (10^{-9} - 10^{-1} M) (main ion) was measured at each addition of the concentration of Fe(II), Zn(II), and Cd(II) (interference ion) solutions. The effect of the presence of interfering ions in the solution is determined by calculating the selectivity coefficient (K_{ij}) using the Nicolski-Eisenman Equation 3 [38,39].

$$K_{ij} = \frac{\left(10^{\frac{\Delta E}{S}} - 1\right) a_i}{a_j}$$ .... (3)

where K_{ij} = selectivity coefficient, S = slope, ΔE = potential value difference, a_i = main ion concentration, and a_j = interfering ion concentration.

Selectivity criteria [38,39]:

• If $a_i > K_{ij} (a_j)^{(n/z)}$ and $K_{ij} = 0 \Rightarrow$ foreign ions do not interfere

• If $K_{ij} < 1$, the electrode is more selective towards i ions than j ions.

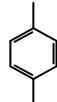• If $K_{ij} > 1$, the electrode is more selective towards j ions than i ions.

3. Results and Discussion

3.1. Characterization of the BEC6ND1 ionophore by FTIR.

Table 1 shows the results of interpreting the BEC6ND1 ionophore FTIR spectrum data. The ester absorption band (RCO$_2$R') appeared at 1761.01 cm^{-1} (vs) (C=O stretch) and 590.22 cm^{-1} (w) (O-C-O bend). The absorption band in the 675 - 575 cm^{-1} range is typical for bending O-C-O esters [29]. The ether absorption band (ROR') appeared at 1292.31 cm^{-1}(s) (C-O-C

stretch in alkyl aryl ethers) and 1066.64 cm^{-1}(s) (R-C-O stretch in alkyl aryl ethers). Aromatic absorption bands (ArH) appeared at 1600.92 cm^{-1} (m) and 1475.54 cm^{-1} (vs) (C=C aromatic ring stretching), 1186.22 cm^{-1} (vs) (C-O aromatic ring stretching), 879.54 cm^{-1} (s) and 821.68 cm^{-1} (s) (Out-of-plane C-H deformation 1,4-disubstituted). Aliphatic absorption bands (RH) appeared at 2958.8 cm^{-1} (vs), 2906.73 cm^{-1} (w), and 2868.15 cm^{-1} (w) (C-H stretch from saturated (CH$_3$)$_3$C-), 1386.82 cm^{-1} (m) (C-H stretch from CH$_3$-), and 1363.67 cm^{-1} (m) (C-H stretch from -CH$_2$-). Thus, the BEC6ND1 ionophore contains ester, ether, aromatic, and aliphatic functional groups.

Table 1. The results of interpreting the FTIR spectrum data of the BEC6ND1 ionophore.

No	Frequency (cm^{-1}) and Intensities	Frequency Ranges (cm^{-1}) and Intensities*	Group or Class	Remarks
1	1761.01 (vs)	1765 - 1720 (vs)	Esters	C=O stretch
2	590.22 (w)	675 - 575 (w)	RCOOR'	O-C-O bend
5	1292.31 (s)	1280 - 1220 (s)	Ethers	C-O-C stretch in alkyl aryl ethers
6	1066.64 (s)	1075 - 1020 (s)	ROR'	R-C-O stretch in alkyl aryl ethers
7	1600,92 (m) 1475,54 (vs)	1630 - 1430 (v)	Aromatic ArH	C=C aromatic ring stretching
8	1186,22 (vs)	1300 - 1000 (s)		C-O aromatic ring stretching
9	879,54 (s)	900 - 650 (s)		Out-of-plane C-H deformation 1,4-disubstituted
10	821,68 (s)			
11	2958,8 (vs)	2970 - 2850 (s)	Aliphatic RH	C-H stretch from saturated (CH$_3$)$_3$C-
12	2906,73 (w)			
13	2868,15 (w)			
14	1386,82 (m)	1450 - 1375 (s)	t-Butil (CH$_3$)$_3$C-	C-H stretch from CH$_3$-
15	1363,67 (m)	1370-1330 (m)	Metilen -CH$_2$-	C-H stretch from -CH$_2$-

∘Notes: vs = *very strong*; v = *variable*; s = *strong*; m = *medium*; w = *weak*.
*Sources: [40-42]

3.2. Nernst (sensitivity) factor of the ISE-BEC6ND1 ionophore.

The results of measuring the potential value of Pb(II) ion at a concentration of 10^{-9} - 10^{-1} M using the ISE-BEC6ND1 ionophore are presented in Table 2. Based on the data in Table 2, Equation 4 is obtained for potential linear regression and Equation 5 for linear regression y over x as follows:

$$E = (533.21 \pm 1.7) + (29.395 \pm 0.1) \log [Pb^{2+}] \quad\quad\quad (4)$$
$$\hat{Y} = (533.21 \pm 1,7) + (29.395 \pm 0,1)\, x \quad\quad\quad (5)$$

Equation 4 shows that the potential value in the linear region decreases as the concentration of Pb(II) metal decreases. Equation 5 shows that the value of the coefficient of the linear regression direction is $[(b) \approx (29.395 \pm 0.1)]$. If x {(-log [Pb(II)]} increases by one unit, then the average ŷ (potential value) decreases (29.395 ± 0.1) mV/decade.

Table 2. The results of measuring the potential value of Pb(II) ion at a concentration of 10^{-9} - 10^{-1} M.

No	Concentration of Pb(II) [M]	-log [Pb(II)]	Potential Value E (mV)
1	10^{-9}	9	275.7
2	10^{-8}	8	295.8
3	10^{-7}	7	328.3

No	Concentration of Pb(II) [M]	-log [Pb(II)]	Potential Value E (mV)
4	10^{-6}	6	353.5
5	10^{-5}	5	379.2
6	10^{-4}	4	413.5
7	10^{-3}	3	447.1
8	10^{-2}	2	475.7
9	10^{-1}	1	507.3
Nernst Factor (S)		29.395 mV/dekade	
E^{o} (K)		533.21	
R^2		0.9973	

The Nernst (sensitivity) factor is the change in analyte concentration and the slope value of the curve obtained at a certain concentration [35]. The sensitivity characteristics can be determined from the linearity curve regression equation. Sensitivity (S) is the slope value (b) of the linear regression Equation (1). The sensitivity value of the ISE-BEC6ND1 ionophore in detecting Pb(II) ions was 29.395 mV/decade (Table 2). These results indicate that the sensitivity of the ISE-BEC6ND1 ionophore is very high because the value of the Nernst factor (S) is the same as the theoretical value (29.6 ± 1.5) mV/decade for divalent ions. These results indicate that the concentration of the BEC6ND1 ionophore (3% w/w) used can increase membrane permeability. Permeability is a membrane performance property that indicates membrane productivity [43-47].

3.3. Limit of detection (LoD) of the ISE-BEC6ND1 ionophore.

Figure 1 shows a linear regression graph of the relationship of -log [Pb(II)] with the potential value of the ISE-BEC6ND1 ionophore. The limit of detection (LoD) is the lowest analyte concentration in a sample that can be consistently detected or measured by the electrode [48-53]. The LoD of the ISE-BEC6ND1 ionophore was determined by constructing an exponential curve on the linear regression lines of the Nernstian and non-Nernstian.
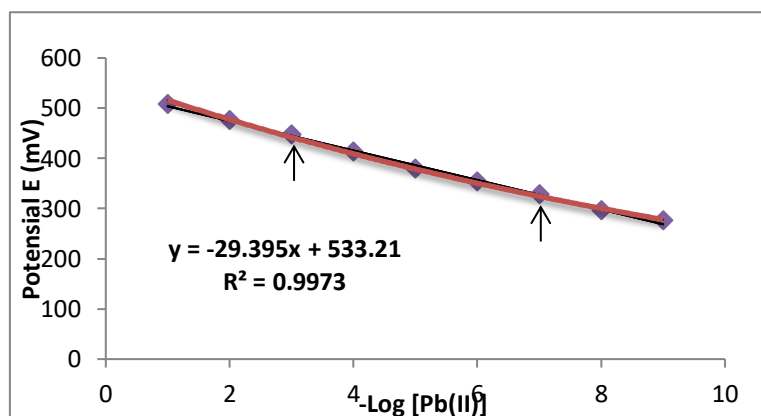

Figure 1. Linear regression graph of the relationship of -log [Pb(II)] with the potential value of the ISE-BEC6ND1 ionophore.

Figure 1 shows that there are two intersection points (sign ↑) of the exponential curve (red line) on the linear regression line (blue line), namely the Pb(II) ion concentrations of 10^{-7} and 10^{-3} M. This indicates that the working concentration of the ISE-BEC6ND1 ionophore is in the ranges of 10^{-7} M (lowest) to 10^{-3} M (highest) so that the LoD of the ISE-BEC6ND1 ionophore is 10^{-7} M. These results indicate that the designed ISE-BEC6ND1 ionophore has a wide linear range and lower detection limit.

Figure 1 also shows the value of the Nernst factor (29.395 mV/decade) and the correlation coefficient (0.9973) of the ISE-BEC6ND1 ionophore. This means that the ISE-BEC6ND1 ionophore is designed with platinum wire 0.2 mm in diameter and 2 cm long as the working electrode, the membrane composition [(BEC6ND1 ionophore : PTCPB : DOS : PVC) (3 : 2 : 60 : 35) % (w/w)], and the properties of the BEC6ND1 ionophores as membrane component materials have a significant effect on the value of the Nernst factor. This is following the statement of Nurdin [54] that the value of the Nernst factor can be influenced by the geometry of the electrode, namely the diameter of the wire in contact with the membrane, the composition of the membrane, and the properties of the membrane component materials. Meanwhile, the thickness of the membrane does not have a significant effect.

3.4. Precision of the ISE-BEC6ND1 ionophore.

Precision is a measure of how well test results can be reproduced. Precision is measured as relative standard deviation (RSD). RSD can be calculated from the data in Table 2 using Equation 1 as follows:

$$RSD = \frac{SD}{\overline{x}} = \frac{80.61}{386.23} = 0.21$$

The result of the above calculation shows that the RSD value of the ISE-BEC6ND1 ionophore is 0.21. The RSD value of 0.21 is less than 2. The smaller the RSD value, the higher the measurement precision of an electrode [55]. This means the ISE-BEC6ND1 ionophore has a very high level of precision or repeatability of the measurement results.

3.5. Response time of the ISE-BEC6ND1 ionophore.

The response time of the ISE-BEC6ND1 ionophores is determined based on the length of time required to produce a constant potential value. The response time was determined by measuring the standard solution of Pb(II) at concentrations between 10^{-9} - 10^{-1} M.

The response time is the time required for an electrode to reach a stable and constant potential value [35]. The response time of the ISE-BEC6ND1 ionophore is approximately 4 - 8 minutes. This means the time required for the ISE-BEC6ND1 ionophore to produce a constant value of potential is 4 - 8 minutes. This response time also indicates the electron transfer rate from the BEC6ND1 ionophore membrane on the electrode surface to Pb(II) ions to provide an accurate measurement response. This means that the higher the concentration of Pb(II) ions in the analyte, the faster the $[R(OCH_2CO_2Et)_6]$ groups of the BEC6ND1 ionophore to interact with the Pb(II) ions to form a complex compound of the $[PbR(OCH_2CO_2Et)_6(NO_3)_2]$.

3.6. Selectivity of the ISE-BEC6ND1 ionophore.

Tables 3, 4, and 5 show the results of measuring the selectivity coefficient (K_{ij}) of the ISE-BEC6ND1 ionophore on the interfering ions Fe(II), Zn(II), and Cd(II).

Table 3. The selectivity coefficient (K_{ij}) of the ISE-BEC6ND1 ionophore on the interfering Fe(II) ions

-log [Fe(II)]	E (mV)	K_{ij}
9	229.5	1.85×10^{-6}
8	278.1	1.55×10^{-5}

-log [Fe(II)]	E (mV)	K_{ij}
7	317.8	1.25×10^{-4}
6	349.2	9.68×10^{-4}
5	373.9	7.40×10^{-3}
4	391.2	4.89×10^{-2}
3	401.7	2.57×10^{-1}
2	407.2	8.71×10^{-1}
1	410.2	2.06×10^{-1}

Table 4. The selectivity coefficient (K_{ij}) of the ISE-BEC6ND1 ionophore on the interfering Zn(II) ions

Table 5. The selectivity coefficient (K_{ij}) of the ISE-BEC6ND1 ionophore on the interfering Cd(II) ions

-log [Zn(II)]	E (mV)	K_{ij}	-log [Cd(II)]	E (mV)	K_{ij}
9	273.1	1.42×10^{-6}	9	234.2	1.73×10^{-6}
8	310.8	1.18×10^{-5}	8	279.9	1.45×10^{-5}
7	340.9	9.24×10^{-5}	7	317.0	1.16×10^{-4}
6	364.5	7.03×10^{-4}	6	346.6	9.07×10^{-4}
5	382.7	5.19×10^{-3}	5	369.8	6.89×10^{-3}
4	396.3	3.63×10^{-2}	4	387.4	4.99×10^{-2}
3	404.5	1.79×10^{-1}	3	398.6	2.81×10^{-1}
2	410.2	9.39×10^{-1}	2	403.9	8.03×10^{-1}
1	413.3	5.46×10^{-1}	1	407.1	8.86×10^{-1}

Tables 3, 4, and 5 show that the average values of the selectivity coefficient (K_{ij}) < 1. The ISE-BEC6ND1 ionophore is highly selective for Pb(II) ions (main ion). This indicates that the presence of the Fe(II), Zn(II), and Cd(II) ions in solution does not interfere with the performance of the ISE-BEC6ND1 ionophore. The results above show that the $[R(OCH_2CO_2Et)_6]$ groups of the BEC6ND1 ionophore are selective against Fe(II), Zn(II), and Cd(II) ions. Selectivity of the BEC6ND1 ionophore toward the Fe(II), Zn(II), and Cd(II) ions related to the nature of hard soft acid bases (HSAB) and the stability of the complex compounds based on the suitability of the size of the metal ions with the ionophore ring size [56,57]. The Fe(II) and Zn(II) ions include acids intermediate so that the Fe(II) and Zn(II) ions cannot interact with the O-carbonyl atom and the O-ether atom, which are soft bases from the $[R(OCH_2CO_2Et)_6]$ groups of the BEC6ND1 ionophore to form complex compounds of the $[FeR(OCH_2CO_2Et)_6(NO_3)_2]$ and $[ZnR(OCH_2CO_2Et)_6(NO_3)_2]$ [58,27].

Although the Cd(II) ion is a soft acid, the Cd(II) ion cannot interact with the O-carbonyl atom and the O-ether atom which is a soft base from the $[R(OCH_2CO_2Et)_6]$ groups of the BEC6ND1 ionophore to form a complex compound of the $[CdR(OCH_2CO_2Et)_6(NO_3)_2]$ [58,27]. This is because the radius of the Cd(II) ion (r = 103 pm) is smaller than the size of the BEC6ND1 ionophore ring, whose radius is ≈ the radius of the K^+ ion (r = 133 pm) [59,60]. On the contrary, although the Pb(II) ion is an intermediate acid, the Pb(II) ion can interact with the O-carbonyl atom and the O-ether atom, which are soft bases from the $[R(OCH_2CO_2Et)_6]$ groups of the BEC6ND1 ionophore to form complex compounds of the $[PbR(OCH_2CO_2Et)_6(NO_3)_2]$ [58,27] (Figure 2 and 3). This is because the Pb(II) ion radius (r = 132 pm) is very close to the size of the BEC6ND1 ionophore ring, whose radius is ≈ the radius of the K^+ ion (r = 133 pm) [59,60]. Figure 3 (b) shows the suitability of the size of the Pb(II) ion radius with the size of the BEC6ND1 ionophore ring.

The process of metal ion reaction with the BEC6ND1 ionophore does not involve the mechanism of ion exchange but through forming a neutral complex with the ion pairs of anionic

salts [61,62]. The formation of complex compounds between Pb(II) ions and the BEC6ND1 ionophore involves nitrate ions as complex ion pairs. The reaction for the formation of this complex does not involve proton exchange. Still, it only involves metal ions Pb(II) as electron-pair acceptors from the oxygen donor from the $[R(OCH_2CO_2Et)_6]$ groups of the BEC6ND1 ionophore. When six molecules of the BEC6ND1 ionophore as ligands donate their lone pairs to the central metal ion Pb(II) to form a coordinating covalent bond, a complex compound of the $[PbR(OCH_2CO_2Et)_6(NO_3)_2]$ is formed. The reaction to form a complex compound of the $[PbR(OCH_2CO_2Et)_6(NO_3)_2]$ between the $[R(OCH_2CO_2Et)_6]$ groups of the BEC6ND1 ionophore and the Pb(II) ion is shown in Figure 2. The 3D structure of a complex compound of the $[PbR(OCH_2CO_2Et)_6(NO_3)_2]$ is shown in Figure 3.
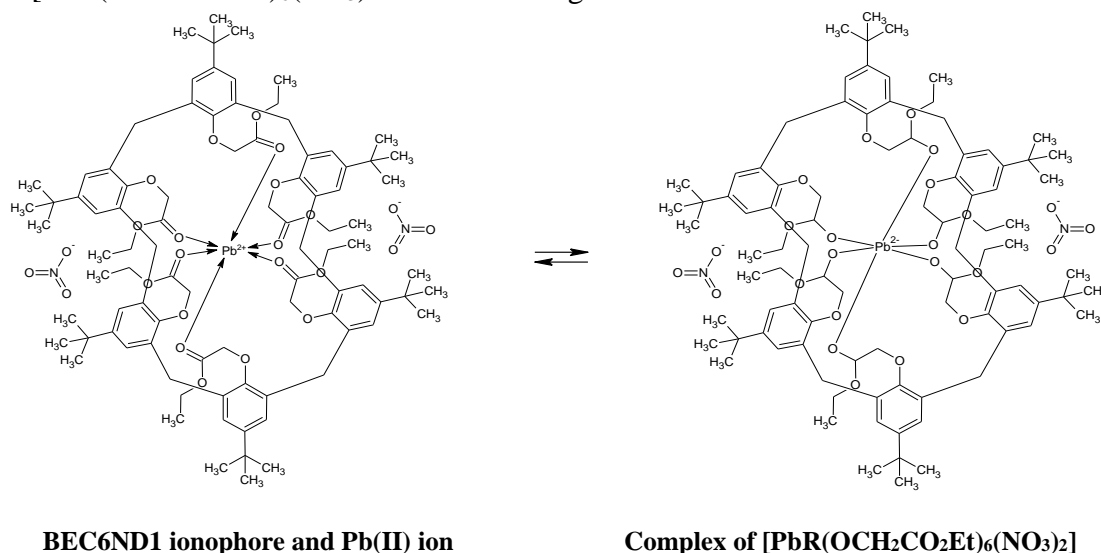

BEC6ND1 ionophore and Pb(II) ion   Complex of [PbR(OCH₂CO₂Et)₆(NO₃)₂]

Figure 2. The reaction for the formation of a complex compound of the $[PbR(OCH_2CO_2Et)_6(NO_3)_2]$ from the $[R(OCH_2CO_2Et)_6]$ groups of the BEC6ND1 ionophore and Pb(II) ions.
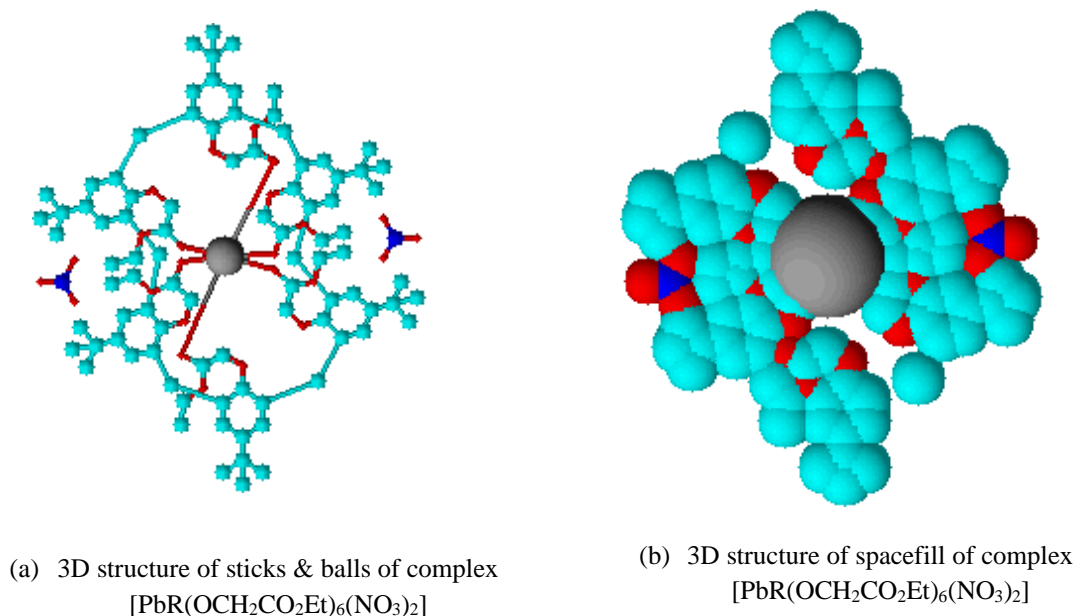

(a) 3D structure of sticks & balls of complex $[PbR(OCH_2CO_2Et)_6(NO_3)_2]$

(b) 3D structure of spacefill of complex $[PbR(OCH_2CO_2Et)_6(NO_3)_2]$

Figure 3. 3D structure of a complex compound of the $[PbR(OCH_2CO_2Et)_6(NO_3)_2]$.

4. Conclusions

The ESI-BEC6ND1 ionophore has good characteristics where it shows a sensitivity value of 29,395 mV/decade, the working concentration range of 10^{-9} - 10^{-1} M, and the limit of

detection (LoD) of 10^{-7} M. The response time is 4 - 8 minutes, with a relative standard deviation (RSD) of 0.21. The ESI-BEC6ND1 ionophore also shows the average value of selectivity coefficient (K_{ij}) < 1. These results indicate that the presence of Fe(II), Zn(II), and Cd(II) ions as interfering ions in the analyte solution does not affect the performance of the ESI-BEC6ND1 ionophores in detecting Pb(II) ions. The ESI-BEC6ND1 ionophore that has been developed shows good selectivity, sensitivity, stability, and reproducibility, so the ESI-BEC6ND1 ionophore is promising to be used as a Pb(II) ion detector in the environment.

Funding

Acknowledgments

Conflicts of Interest

The authors declare no conflict of interest.

References

1. Darmono. Metals in Living Biological Systems; UI Press: Jakarta, Indonesia, **1995**; pp. 5.
2. Darmono. Environment and Pollution; UI Press: Jakarta, Indonesia, **2006**; pp. 13.
3. Palar, H. Heavy Metal Pollution and Toxicology; Rineka Cipta: Jakarta, Indonesia, **2008**; pp.17.
4. Jiang, L.; Mo, G.; Chunhe Yu, C.; Ya, D.; He, X.; Mo, W.; Deng, B. Based on Reduced Graphene Oxide-Copper Sulfide-Carbon Nitride Nanosheets Composite Electrochemiluminescence Sensor for Determination of Gatifloxacin in Mouse Plasma. *Colloids and Surfaces B: Biointerfaces* **2019**, *173*, pp. 378-385, https://doi.org/10.1016/j.colsurfb.2018.10.003
5. Yang, P.; Zhou, R.; Zhang, W.; Yi, R.; Tang, S.; Guo, L.; Hao, Z.; Li, X.; Lu, Y.; Zeng, X. High-Sensitivity Determination of Cadmium and Lead in Rice Using Laser Induced Breakdown Spectroscopy. *Food Chem* **2019**, *272*, pp. 323-328, https://doi.org/10.1016/j.foodchem.2018.07.214
6. Li, G.; Qi, X.; Zhang, G.; Wang, S.; Li, K.; Wu, J.; Wan, X.; Liu, Y.; Li, Q. Low Cost Voltammetric Sensors for Robust Determination of Toxic Cd(II) and Pb(II) in Environment and Food Based on Shuttle Like α-Fe_2O_3 Nanoparticles Decorated β-Bi_2O_3 Microspheres. *Microchem. J.* **2022**, *179*, pp. 107515, https://doi.org/10.1016/j.microc.2022.107515
7. Wang, Y.; Wu, X.; Sun, J.; Wang, C.; Zhu, G.; Bai, L.P.; Jiang, Z.H.; Zhang, W. Stripping Voltammetric Determination of Cadmium and Lead Ions Based on a Bismuth Oxide Surface Decorated Nanoporous Bismuth Electrode. *Electrochemistry Communications* **2022**, *136*, pp. 107233, https://doi.org/10.1016/j.elecom.2022.107233
8. Xu, X.; Yang, S.; Wang, Y.; Qian, K. Nanomaterial Based Sensors and Strategies for Heavy Metal Ion Detection. *Green Anal. Chem.* **2022**, *2*, pp. 100020, https://doi.org/10.1016/j.greeac.2022.100020
9. Kazantzi, V.; Drosaki, E.; Skok, A.; Vishnikini, A.B.; Anthemidis, A. Evaluation of Polypropylene and Polyethylene as Sorbent Packing Materials in Online Preconcentration Columns for Trace Pb(II) and Cd(II) Determination by FAAS. *Microchem. J* **2019**, *148*, pp. 514-520, https://doi.org/10.1016/j.microc.2019.05.033
10. Kheirandish, S.; Ghaedi, M.; Dashtian, K.; Jannesar, R.; Montazerozohori, M.; Pourebrahim, F.; Zare, M.A. Simultaneous Removal of Cd(II), Ni(II), Pb(II) and Cu(II) Ions via Their Complexation with HBANSA Based on a Combined Ultrasound-assisted and Cloud Point Adsorption Method Using CSG-$BiPO_4$/$FePO_4$ as Novel Adsorbent: FAAS Detection and Optimization Process. *J. Colloid Interface Sci.* **2017**, *500*, pp. 241-252, https://doi.org/10.1016/j.jcis.2017.03.070
11. Jose, M.; Prakash, P.; Jeyaprabha, B.; Ibrahim, R.; Mathew, R.M.; Zakaria, E.S.; Thomas, V.; Thomas, J. Principle, Design, Strategies, and Future Perspectives of Heavy Metal Ion Detection Using Carbon Nanomaterial-Based Electrochemical Sensors: a Review. *J. Iran. Chem. Soc.* **2023**, *20*, pp. 775-791,

https://doi.org/10.1007/s13738-022-02730-5

12. Alothman, Z.A.; Yilmaz, E.; Habila, M.A.; Alsohaimi, I.H.; Aldawsari, A.M.; AL-Harbi, N.M.; Soylak, M. Triethylenetetramine Modified Multiwalled Carbon Nanotubes for The Efficient Preconcentration of Pb(II), Cu(II), Ni(II) and Cd(II) Before FAAS Detection. *RSC Advances* **2015**, *5(129)*, pp. 106905-106911, https://doi.org/10.1039/c5ra19213g

13. Yang, K.; Yang, X.; Liu, E.; Shi, C.; Ma, L.; He, C.; Li, Q.; Li, J.; Zhao, N. Elevated Temperature Compressive Properties and Energy Absorption Response of in-situ Grown CNT-Reinforced Al Composite Foams. *Mater. Sci. Eng.: A* **2017**, *690*, pp. 294-302, https://doi.org/10.1016/j.msea.2017.03.004

14. Wang, X.; Guo, H.; Yin, F.; Tu, Y. A Glucose Biosensor Based on Prussian Blue/Chitosan Hybrid Film. *Biosensors and Bioelectronics* **2009**, *24(1)*, pp. 1527–1530, https://doi.org/10.1016/j.bios.2008.09.025

15. Nisah, K.; Ramli, M.; Marlina; Idroes, R.; Safitri, E. Study of Linearity and Stability of Pb(II)-1,10-Phenanthroline Complex with The Presence of Fe (II) and Mg (II) Matrix Ions Using UV-Vis Spectrophotometry. *IOP Conf. Ser. Mater. Sci. Eng.* **2021**, *1087*, pp .1-7, https://doi.org/10.1088/1757-899X/1087/1/012052

16. Zhao, G.; Wang, H.; Liu, G. Sensitive Determination of Trace Cd(II) and Pb(II) in Soil by an Improved Stripping Voltammetry Method Using Two Different *in situ* Plated Bismuth-Film Electrodes Based on a Novel Electrochemical Measurement System. *RSC Adv.* **2018**, *8*, pp. 5079-5089, https://doi.org/10.1039/C7RA12767G

17. Tormin, T.F.; Oliveira, G.K.F.; Richter, E.M.; Munoz, R.A.A. Voltammetric Determination of Pb, Cu and Hg in Biodiesel Using Gold Screen-printed Electrode: Comparison of Batch-injection Analysis with Conventional Electrochemical Systems. *Electroanalysis* **2016**, *28(5)*, pp. 940-946, https://doi.org/10.1002/elan.201501012

18. Pérez-Ràfols, C.; Serrano, N.; Díaz-Cruz, J.M.; Ariño, C.; Esteban, M. Penicillamine Modified Sensor for The Voltammetric Determination of Cd(II) and Pb(II) Ions in Natural Samples. *Talanta* **2015**, *144*, pp. 569-573, https://doi.org/10.1016/j.talanta.2015.06.083

19. Ozbek, O.; Gezegen, H.; Cetin, A.; Isildak, O. A Potentiometric Sensor for the Determination of Pb(II) Ions in Different Environmental Samples. *Chemistry Select* **2022**, *7(33)*, pp. 75-83, https://doi.org/10.1002/slct.202202494

20. Jaber, L.; Elgamouz, A.A; Kawde, A.N. An Insight to the Filtration Mechanism of Pb(II) at the Surface of a Clay Ceramic Membrane Through its Preconcentration at the Surface of a Graphite Clay Composite Working Electrode. *Arabian Journal of Chemistry* **2022**, *15(12)*, pp. 104303, https://doi.org/10.1016/j.arabjc.2022.104303

21. Moustafa, E.M.I.; Amin, A.S.; El-Attar, M.A. A Highly Selective Bulk Optode Based on 6-{4-(2,4-Dihydroxy-Phenyl)Diazenyl)Phenyl}-2-Oxo-4-Phenyl-1,2-Dihydro-Pyridine-3-Carbonitrile Incorporating Chromoionophore V for Determination of Nano Levels of Cadmium. *Analytical Biochemistry* **2022**, *654*, pp. 114835, https://doi.org/10.1016/j.ab.2022.114835

22. Masykur, A.; Noviandri, I.; Buchari. Lifespan and Effect of Oxidizing Reducing Potential on Electrode Potential Hydrogen Ion Selective (ESI) with Antimony Active Ingredients. *AlChemy Jurnal Penelitian Kimia* **2002**, *1(2)*, pp. 7-19.

23. Bailey, L.P. Analysis with Selective Electrodes; Heiden & Sons, Ltd.: New York, **1996**; pp. 451.

24. Wahab, A.W. The Effect of PVC-Based Membrane Composition and Zn(II), Cd(II) and Pb(II) Interfering Ions to Hg(II) Ion Selective Electrode (ISE) Performance by Using DBA$_2$18C6 Ionophore. *Indonesian Journal of Chemistry* **2006**, *6(1)*, pp. 27-31, https://doi.org/10.22146/ijc.21768

25. Dali, N.; Wahab, A.W.; Firdaus, Z.; Maming, M.; Nurdin, M. Synthesis of Hexa(*p-tert-*butyl)hexa(carboxylicacid)calix[6]arene from Hexa(*p-tert-*butyl)hexa(ethylester)calix[6]arene. *Int. J. ChemTech Res.* **2016**, *9(7)*, pp. 486-490.

26. Awaluddin, I.P.; Wahab, A.W.; Maming. Ion Selective Electrode Design for Metal Lead(II) [(ISE-Pb(II)] Using Ionophores *p-tert-*Butylcalix[4]arene. *Al-Kimia Journal of Chemistry* **2015**, *3(1)*, pp. 24-33, https://doi.org/10.24252/al-kimia.v3i1.1658

27. Dali, N. Synthesis, Characterization, and Application of Derivatives Compound of the Thioamide p-tert-Butylcalix[4]-and-[6]arene as Ionophores on Ion Selective Electrode (ISE) Coated Wire Type for Heavy Metal Content Analysis Hg(II) and Au(I). Dissertation, Hasanuddin University, Makassar, Indonesia, **October 26**, **2016**.

28. Dali, N.; Dali, S.; Chairunnas, A.; Amalia, H.A.M.; Puspitasari, S.A.A. Synthesis of the BETAC4ND5 Ionophore from *p-t*-Butylcalix[4]arene Ethylesteramide. *AIP Conf. Proc.* **2022**, *2638(1)*, pp. 060005-1 - 060005-10, https://doi.org/10.1063/5.0104714

29. Dali, N.; Dali, S.; Chairunnas, A.; Amalia, H.A.M.; Puspitasari, S.A.A. Highly Selective and Sensitive Determination of Hg(II) Ions Using Ion Selective Electrodes (ISE) Coated With The BEC4ND1 Ionophore as Membranes. *JKPK* **2022**, *7(2)*, pp. 242-254, https://doi.org/10.20961/jkpk.v7i2.62213

30. Muzakkar, M.Z.; Maulidiyah, M.; Aziz, T.; Nurdin, M.; Natsir, M.; Dali, N.; Ratna. Performance of Selenium Doped TiO$_2$/Ti Composite Electrodes (Se-TiO$_2$/Ti): Photoelectrocatalyst of Reactive Green 19 under UV-Visible Irradiation. *AIP Conf. Proc.* **2022**, *2638(1)*, pp. 020004-1–020004-11, https://doi.org/10.1063/5.0109569

31. Dali, N.; Deriatman, D.; Arham, Z.; Irwan, I.; Mustapa, F.; Maulidiyah, M.; Nurdin, M. Electrochemical Performance of Graphene Paste Electrode Modified TiO$_2$-Calix[4]arene (G@TC) as a Cd^{2+} Ion Detection. *AIP Conf. Proc.* **2023**, *2719(1)*, pp. 030011-1 - 030011-6, https://doi.org/10.1063/5.0133281

32. Dali, N.; Amasi, A.A.; Irwan, I.; Mustafa, F.; Maulidiyah, M.; Nurdin, M. Highly Sensitive Determination of Pb(II) Ions Using Graphene Paste Electrode Modified TiO$_2$-Ionophore Calix[6]arene Composite. *AIP Conf. Proc.* **2023**, *2719(1)*, pp. 030015-1 - 030015-8, https://doi.org/10.1063/5.0133282

33. Dali, N.; Dali, S.; Chairunnas, A.; Amalia, H.A.M.; Puspitasari, S.A.A. Synthesis of Ionophore from *p-t*-Butyl(carboxymethoxy)calix[4]arene Substituted Amide. *Molekul* **2023**, *18(1)*, pp. 50-58, https://doi.org/10.20884/1.jm.2023.18.1.5927

34. Dali, N.; Wahab, A.W.; Firdaus; Maming. Synthesis of hexa-*p-tert*-butylhexaestercalix[6]arene from *p-tert*-butylcalix[6]arene, *Al-Kimia Journal of Chemistry* **2015**, *3(1)*, pp. 103-109, https://doi.org/10.24252/al-kimia.v3i1.1665

35. Bigman, J.L.; Reinhardt, K.A. Monitoring of Chemicals and Water, Handbook of Silicon Wafer Cleaning Technology; Elsevier Inc.: CA, USA, **2018**; pp. 259, https://doi.org/10.1016/B978-0-323-51084-4.00011-3

36. Christian, G.D.; Dasgupta, P.K.; Schug, K.A. Analytical Chemistry; John Wiley & Sons: NY, USA, **2013**; pp. 357, https://books.google.co.id/books?id=AohqtwAACAAJ&printsec=frontcover&hl=id&source=gbs_ge_summary_r&cad=0#v=onepage&q&f=false

37. Mark, H.; Workman, J. Chapter 72 - Limitations in Analytical Accuracy: Part 1—Horwitz's Trumpet; Academic Press: CA, USA, **2018**, pp. 491, https://doi.org/10.1016/b978-0-12-805309-6.00072-6

38. Deyhimi, F. A Method for the Determination of Potentiometric Selectivity Coefficients of Ion Selective Electrodes in the Presence of Several Interfering Ions. *Talanta* **1999**, *50(5)*, pp. 1129-34, https://doi.org/10.1016/s0039-9140(99)00194-0

39. Dali, N.; Dali, A.; Dali, S.; Amalia, H.A.M. Synthesis of the BEAC4ND4 Ionophore from *p-t*-Butylcalix[4]arene Carboxylic Acid. *JKSA* **2020**, *23(12)*, pp. 424-431, https://doi.org/10.14710/jksa.23.12.424431

40. Jain, V.K.; Pillap, S.G.; Mandal, H.C. Liquid-Liquid Extraction, Preconcentration and Transport Studies of Lanthanum(III) with Calix [4] Resorcinarene-Hydroxamic Acid (C4RAHA). *J. Chil. Chem. Soc.,* **2007**, *52(2)*, pp. 1177-1181, https://dx.doi.org/10.4067/S0717-97072007000200013

41. Lambert, J.B.; Gronert, S.; Shurvell, H.F.; Lightner, D.A. Organic Structural Spectroscopy; Pearson Prentice Hall: New York, USA, **2011**, pp. 342.

42. Kemp, W. Organic Spectroscopy; MacMillan Education Ltd.: London, Inggris, **1991**, pp. 58, https://doi.org/10.1007/978-1-349-15203-2

43. Sastrohamidjojo, H. Nuclear Magnetic Resonance Spectroscopy; Liberty: Yogyakarta, Indonesia, **1994**, pp. 68.

44. Arham, Z.; Kurniawan, K.; Anhusadar, L. High Electrochemical Response of TiO$_2$@C-Dots Nanocomposites as Electrode Modifiers for Pb (II) Detection. *Materials Science in Semiconductor Processing* **2023**, *160*, pp. 107466, https://doi.org/10.1016/j.mssp.2023.107466

45. Galinski, B.; Wysiecka, E.W. Pyrrole Bearing Diazocrowns: Selective Chromoionophores for Lead(II) Optical Sensing. *Sensors and Actuators B: Chemical* **2022**, *361*, pp. 131678, https://doi.org/10.1016/j.snb.2022.131678

46. Azam, N.; Habib, S.I.; Madoo, M.A.W. Fabrication and Characterization of Novel Pb(II) and Cr(III) Ion Selective and Sensitive Electrodes. *Elec. J. Chem.* **2022**, *3(4)*, pp. 16-25, https://dx.doi.org/10.24018/ejchem.2022.3.4.119

47. Malik, L.A.; Pandith, A.H.; Bashir, A.; Qureashi, A. Zinc Oxide Decorated Multiwalled Carbon Nanotubes: a Selective Electrochemical Sensor for the Detection of Pb(II) Ion in Aqueous Media. *Journal of Materials Science: Materials in Electronics* **2022**, *9*, pp. 105678, https://doi.org/10.1016/j.matsci.2022.105678

48. Cetinkaya, A.; Yıldız, E.; Kaya, S.I.; Corman, M.E.; Uzun, L.; Ozkan, S.A. A Green Synthesis Route to Develop Molecularly Imprinted Electrochemical Sensor for Selective Detection of Vancomycin from Aqueous and Serum Samples. *Green Anal. Chem.* **2022**, *2*, pp. 100017, https://doi.org/10.1016/j.greeac.2022.100017

49. Cetinkaya, A.; Kaya, S.I.; Corman, M.E.; Karakaya, M.; Atici, E.B.; Ozkan, S.A. A Highly Sensitive and Selective Electrochemical Sensor Based on Computer Aided Design of Molecularly Imprinted Polymer for the Determination of Leflunomide. *Microchem. J.* **2022**, *179*, pp. 107496, https://doi.org/10.1016/j.microc.2022.107496

50. Azimi, H.; Sullivan, C.; Lu, D.; Brack, E.; Drew, C.; Kurup, P. Voltammetric Determination of Trace Methyl Parathion using Electrochemically Reduced Graphene Oxide Modified Carbon Screen-Printed Electrodes. *Anal. Bioanal. Electrochem.* **2023**, *15(5)*, pp. 356-370, https://doi.org/10.22034/ABEC.2023.705134

51. Wibowo, D.; Sari, W.O.S.I.; Said, A.; Mustapa, F.; Susianti, B.; Maulidiyah, M.; Nurdin, M. Electrochemical-Sensor Behavior for Determination of Low Urea Concentration using Graphite-TiO2 Composites Immobilized in a Glass Tube. *Anal. Bioanal. Electrochem.* **2022,** *14(4)*, pp. 385-401, https://www.abechem.com/article_252040_cdd6f0155294f7650946a1627aa58ed1.pdf

52. Pourbasheer, E. High Accurate Prediction of Carbonate Selectivity of PVC-Plasticized Membranes Sensors by Genetic Algorithm-Support Vector Machine. *Anal. Bioanal. Electrochem.* **2023**, *15(2)*, pp. 150-165, https://doi.org/10.22034/ABEC.2023.702332

53. Kamal, N. Effect of CMC (Carboxyl Methyl Cellulose) Additives Against Some Parameters in the Solution Sucrose. *J. Technology* **2010**, *1(17)*, pp. 78–84, http://lib.itenas.ac.id/kti/wp-content/uploads/2014/04/JURNAL-Netty-Kamal-ED-17.pdf

54. Vashist, S.K.; Luong, J.H.T. Bioanalytical Requirements and Regulatory Guidelines for Immunoassays: Handbook of Immunoassay, Technologies, Approaches, Performances, and Applications; Elsevier Inc.: CA, USA, **2018**, pp. 75, https://doi.org/10.1016/B978-0-12-811762-0.00004-9

55. Nurdin, M.; Dali, N.; Irwan, I.; Maulidiyah, M.; Arham, Z.; Ruslan, R.; Hamzah, B.; Sarjuna, S.; Wibowo, D. Selectivity Determination of Pb^{2+} Ion Based on TiO$_2$-Ionophores BEK6 as Carbon Paste Electrode Composite. *Anal. Bioanal. Electrochem* **2018**, *10(12)***,** pp. 1538-1547.

56. Mashuni, M.; Ritonga, H.; Jahiding, M.; Hamid, F.H. Chitosan Synthesis from Skin Shrimp as a Membrane Material Au/Chitosan/GTA/AChE electrode for Pesticide Detection. *AlChemy Jurnal Penelitian Kimia* **2022**, *18(1)*, pp. 112-121, https://doi.org/10.20961/alchemy.18.1.56551.112-121

57. Maming, Transport Cr(III), Cd(II), Pb(II) and Ag(I) Through the Bulk Liquid Membrane Containing Derivative Carboxylic, Ester, and Amide *p-tert*-Butylcalix[4]arene as Ion Carrier. Dissertation, Gadjah Mada University, Yogyakarta, Indonesia, **October 26, 2008**.

58. Kadir, A.N. Transport Selectivity Calix[4]arene and Calix[6]arene Carboxylates Against Fe^{3+} of Mixture of Fe, Ni, and Cr Through 1,2-Dichloroethane Bulk Liquid Membrane. *Scientific Journal dr. Aloei Saboe* **2014**, *1(2)*, pp. 1-6.

59. Huheey, J.E. Inorganic Chemistry: Principles of Structure and Reactivity; Harper International SI Edition: Cambridge, Inggris, **1983**, pp. 312.

60. J. Emsley, The Elements, Clarendon Press: Oxford, USA, **1989**, pp. 102.

61. Gutsche, C.D. Calixarenes Revised; Stoddart, J.F., Editor. The Royal Society of Chemistry: New York, USA, **1998**, pp. 75, https://doi.org/10.1039/9781847550293

62. Maming; Jumina, D.; Siswanta; Sastrohamidjojo, H. Transport of Cr^{3+}, Cd^{2+}, Pb^{2+}, and Ag$^+$ Ions Through Bulk Liquid Membrane Containing p-tert-Butylcalix[4]arene Tetracarboxylic Acid as Ion Carrier. *Indo. J. Chem.* **2007**, *7(1)*, pp. 172-179, https://doi.org/10.22146/ijc.21694